Evaluation of Irrigant Flow in the Root Canal Using Different Needle Types by an Unsteady Computational Fluid Dynamics Model

Christos Boutsioukis, DDS, MSc,[*†] *Bram Verhaagen, MSc,*[‡] *Michel Versluis, PhD,*[‡] *Eleftherios Kastrinakis, PhD,*[§] *Paul R. Wesselink, DDS, PhD,*[†] *and Lucas W.M. van der Sluis, DDS, PhD*[†]

Abstract

Introduction: The aim of this study was to evaluate the effect of needle tip design on the irrigant flow inside a prepared root canal during final irrigation with a syringe using a validated Computational Fluid Dynamics (CFD) model. **Methods:** A CFD model was created to simulate the irrigant flow inside a prepared root canal. Six different types of 30-G needles, three open-ended needles and three close-ended needles, were tested. Using this CFD model, the irrigant flow in the apical root canal was calculated and visualized. As a result, the streaming velocity, the apical pressure, and the shear stress on the root canal wall were evaluated. **Results:** The open-ended needles created a jet toward the apex and maximum irrigant replacement. Within this group, the notched needle appeared less efficient in terms of irrigant replacement than the other two types. Within the close-ended group, the side-vented and double side-vented needle created a series of vortices and a less efficient irrigant replacement; the side-vented needle was slightly more efficient. The multi-vented needle created almost no flow apically to its tip, and wall shear stress was concentrated on a limited area, but the apical pressure was significantly lower than the other types. **Conclusions:** The flow pattern of the open-ended needles was different from the close-ended needles, resulting in more irrigant replacement in front of the open-ended needles but also higher apical pressure. *(J Endod 2010;36:875–879)*

Key Words

Computational Fluid Dynamics, irrigation, needle, tip

The irrigation of root canals with antibacterial solutions is considered an essential part of chemomechanical preparation (1). Irrigation with a syringe and a needle remains the most commonly used procedure (2, 3). However, there is an uncertainty about the efficiency of this procedure in the apical part of the root canal (4–6).

To increase the efficiency of syringe irrigation, different needle types have been proposed (7–13). Previous studies of the resulting flow (7, 8, 10, 12) were limited because an indirect or a macroscopic approach can only provide a coarse and incomplete estimation of the irrigant flow. Consequently, there is still no consensus on the superiority of any of these types.

Computational Fluid Dynamics (CFD) represents a powerful tool to investigate flow patterns by mathematical modeling and computer simulation (14, 15). CFD simulations can provide details of the velocity field, shear stress, and pressure in areas in which experimental measurements are difficult to perform. Recently, a CFD model was proposed for the evaluation of irrigant flow in the root canal (16) and was subsequently validated by comparison with experimental high-speed imaging data (17). The aim of this study was to evaluate the effect of needle tip design on the apical irrigant flow inside a prepared root canal during final irrigation with a syringe using this validated CFD model.

Materials and Methods

The root canal and apical anatomy were simulated similarly to a previous study (16), assuming a length of 19 mm, an apical diameter of 0.45 mm (ISO size 45), and 6% taper. The apical foramen was simulated as a rigid and impermeable wall.

Six different needle types were modeled using commercially available 30-G needles as a reference (Fig. 1). The needle types can be divided in two main groups: open-ended (Fig. 1*A-C*) and close-ended (Fig. 1*D-F*). The external and internal diameter and the length of all needles were standardized (D_{ext} = 320 μm, D_{int} = 196 μm, l = 31 mm, respectively) in order to isolate the effect of needle tip design. These values correspond closely to the real geometry of the needles, which was determined according to a previous study (18). The two outlets of the double side-vented needle were modeled identical to the outlet of the side-vented needle to exclude the possible effect of the outlet design. The needles were fixed and centered within the canal, 3 mm short of the working length (WL).

From the *Department of Endodontology, Dental School, Aristotle University of Thessaloniki, Thessaloniki, Greece; †Department of Cariology, Endodontology, Pedodontology, Academic Centre for Dentistry Amsterdam, Amsterdam, The Netherlands; ‡Physics of Fluids Group, Faculty of Science and Technology and Research Institute for Biomedical Technology and Technical Medicine MIRA, University of Twente, Enschede, The Netherlands; and §Chemical Engineering Department, School of Engineering, Aristotle University of Thessaloniki, Thessaloniki, Greece.

Supported in part through a Scholarship for Excellent PhD Students from the Research Committee of Aristotle University of Thessaloniki, Greece (CB) and through Project 07498 of the Dutch Technology Foundation STW (BV).

Address requests for reprints to Mr Christos Boutsioukis, 29, Kimis Street, 551 33 Thessaloniki, Greece. E-mail address: chb@dent.auth.gr.

0099-2399/$0 - see front matter

doi:10.1016/j.joen.2009.12.026

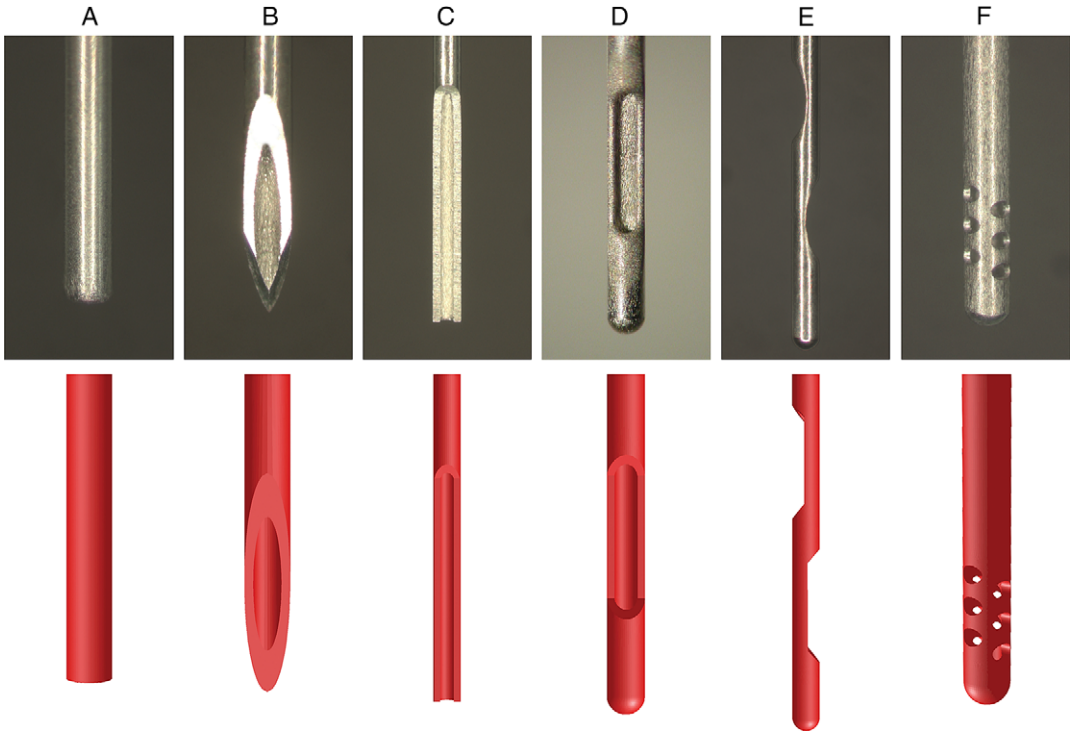

Figure 1. Commercially available 30-G needles used as references (top) and corresponding three-dimensional models created (bottom). (*A-C*) Open-ended needles: (*A*) flat (NaviTip; Ultradent, South Jordan, UT), (*B*) beveled (PrecisionGlide Needle; Becton Dickinson & Co, Franklin Lakes, NJ), and (*C*) notched (Appli-Vac Irrigating Needle Tip; Vista Dental, Racine, WI). (*D-F*) Close-ended needles: (*D*) side-vented (KerrHawe Irrigation Probe; KerrHawe SA, Bioggio, Switzerland), (*E*) double side-vented (Endo-Irrigation Needle; Transcodent, Neumünster, Germany), and (*F*) multi-vented (EndoVac Microcannula; Discus Dental, Culver City, CA). Variable views and magnification were used to highlight differences in tip design.

The preprocessor Gambit 2.4 (Fluent Inc, Lebanon, NH) was used to build the 3-dimensional geometry and the mesh. A hexahedral mesh was constructed, and a grid refinement was performed near the walls and in areas in which high gradients of velocity were anticipated. A grid-independency check was performed to ensure the reasonable use of computational resources. The final meshes consisted of 597,400 to 810,600 cells depending on needle type (mean cell volume = 2.07-2.82 $\cdot$ 10^{-5} mm^3).

No-slip boundary conditions were applied under the hypothesis of rigid, smooth, and impermeable walls. The fluid flowed into the simulated domain through the needle inlet and out of the domain through the root canal orifice where atmospheric pressure was imposed. The root canal and needle were assumed to be completely filled with the irrigant. A flat velocity profile with a constant axial velocity of 8.6 m/s was imposed at the needle inlet, which is consistent with a clinically realistic irrigant flow rate of 0.26 mL/s through a 30-G needle (19). The irrigant, sodium hypochlorite 1%, was modeled as an incompressible Newtonian fluid, with density ρ = 1.04 g/cm^3 and viscosity $\mu = 0.99 \cdot 10^{-3}$ Pa$\cdot$s (16). Gravity was included in the flow field in the direction of the negative z axis.

The commercial CFD code FLUENT 6.3 (Fluent Inc) was used to set up and solve the problem. Detailed settings of the solver can be found in another study (17). Computations were performed in a computer cluster (45 dual-core AMD Opteron 270 processors) running 64-bit SUSE Linux 10.1 (kernel version 2.6.16). The flow fields for the six needle types were calculated and compared in terms of velocity, shear stress, and apical pressure.

Results

Of the open-ended needles, the flat and beveled needle presented similar high-velocity jets of irrigant in the root canal (Fig. 2.1*A* and *B*). For the notched needle, the velocities in the jet were slightly lower (Fig. 2.1*C*). The flow pattern of the close-ended needles was different compared with the open-ended needles. The flow was more directed to the root canal wall in place of the apex. The side-vented and double side-vented needle presented a flow pattern with a jet of irrigant formed at the outlet (the one proximal to the tip for the double side-vented) and directed toward the apex with a divergence of approximately 30° (Fig. 2.1*D-E*). The irrigant followed a curved path around the tip. A series of three counter-rotating vortices were identified apically to the tip. The irrigant flowing out of the proximal outlet of the double side-vented needle amounted to 93.5% of the total flow. As a result, the flow from the distal outlet presented only a minor influence on the flow pattern.

Several small jets were formed by the irrigant exiting the multi-vented needle from the six outlets proximal to the tip (Fig. 2.1*F*). The most intense jets were formed through the most proximal pair of outlets, which was responsible for 73% of the total flow, whereas the second and third pair of outlets were responsible for 25% and 2%, respectively. The other three pairs of outlets did not contribute to the outflow. Very low velocities were noted apically to the tip.

Streamlines indicating the route of massless particles released downstream from the needle inlet depicted the main flow of the delivered irrigant in three dimensions (Fig. 2.2). Analysis of the axial z component of irrigant velocity in the apical part of the canal as a function of the distance from the WL (Fig. 3.1) provided a more detailed overview of irrigant replacement, which was considered clinically significant for velocities >0.1 m/s. The replacement of irrigant extended further than 2 mm apically to the tip of the open-ended needles, whereas it was limited within 1 to 1.5 mm apically to the tip of the close-ended needles.

The shear stress pattern on the canal wall was similar between the flat, beveled, and notched needle, but the beveled and notched types

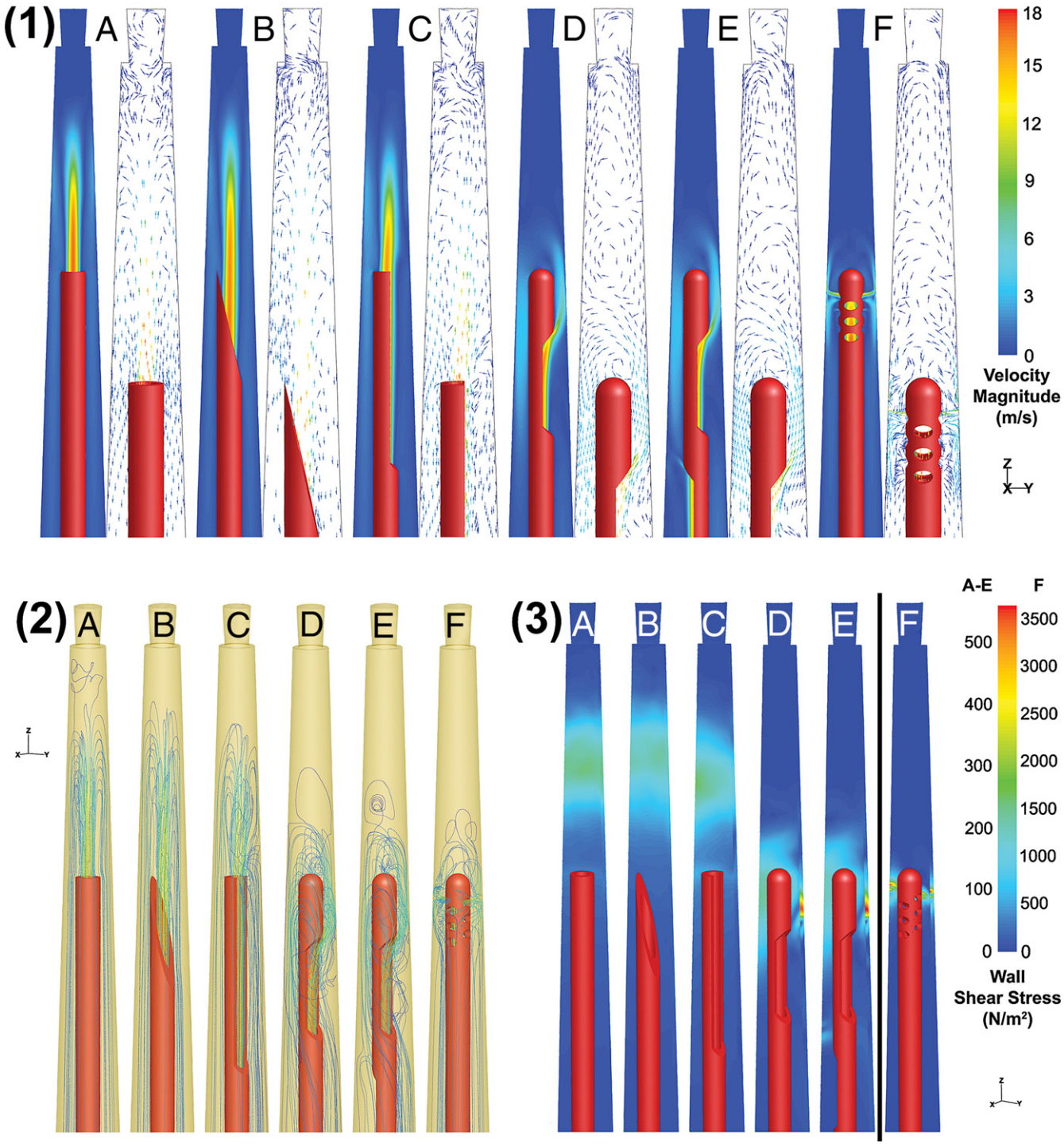

Figure 2. (1) Time-averaged contours of velocity magnitude (left) and vectors (right) along the *z-y* plane in the apical part of the root canal. Within 2.5 mm, the jets formed by the (*A*) flat, (*B*) beveled, and (*C*) notched needles appeared to break up gradually because of damping by the irrigant already present in the canal. The reverse flow toward the canal orifice was noted mainly near the canal wall. The (*D*) side-vented and (*E*) double side-vented needles presented a jet of irrigant formed at the outlet (the one proximal to the tip for the double side-vented) and directed toward the apex with a divergence of approximately 30°. The irrigant followed a curved path around the tip and was finally directed toward the canal orifice. A series of counter-rotating vortices was noted apically to the tip. The velocity of the fluid inside each vortex decreased 5- to 10-fold toward the apex. (*F*) Several small jets were formed by the irrigant exiting the multi-vented needle from the six outlets proximal to the tip. The jets were directed perpendicular to the canal wall and then toward the canal orifice, whereas a small part followed a path around the tip. (2) Streamlines indicating the route of massless particles released downstream from the needle inlet and colored according to time-averaged velocity magnitude. Particle trajectories provide visualization of the fresh irrigant main flow in three dimensions. Both presence and density of the streamlines are important to indicate the degree of irrigant penetration. Irrigant flow coronally to the tip showed complete replacement irrespective of needle tip design. (3) Time-averaged distribution of shear stress on the root canal wall. Only half of the root canal wall is presented to allow simultaneous evaluation of the needle position. Needles are coloured in red.

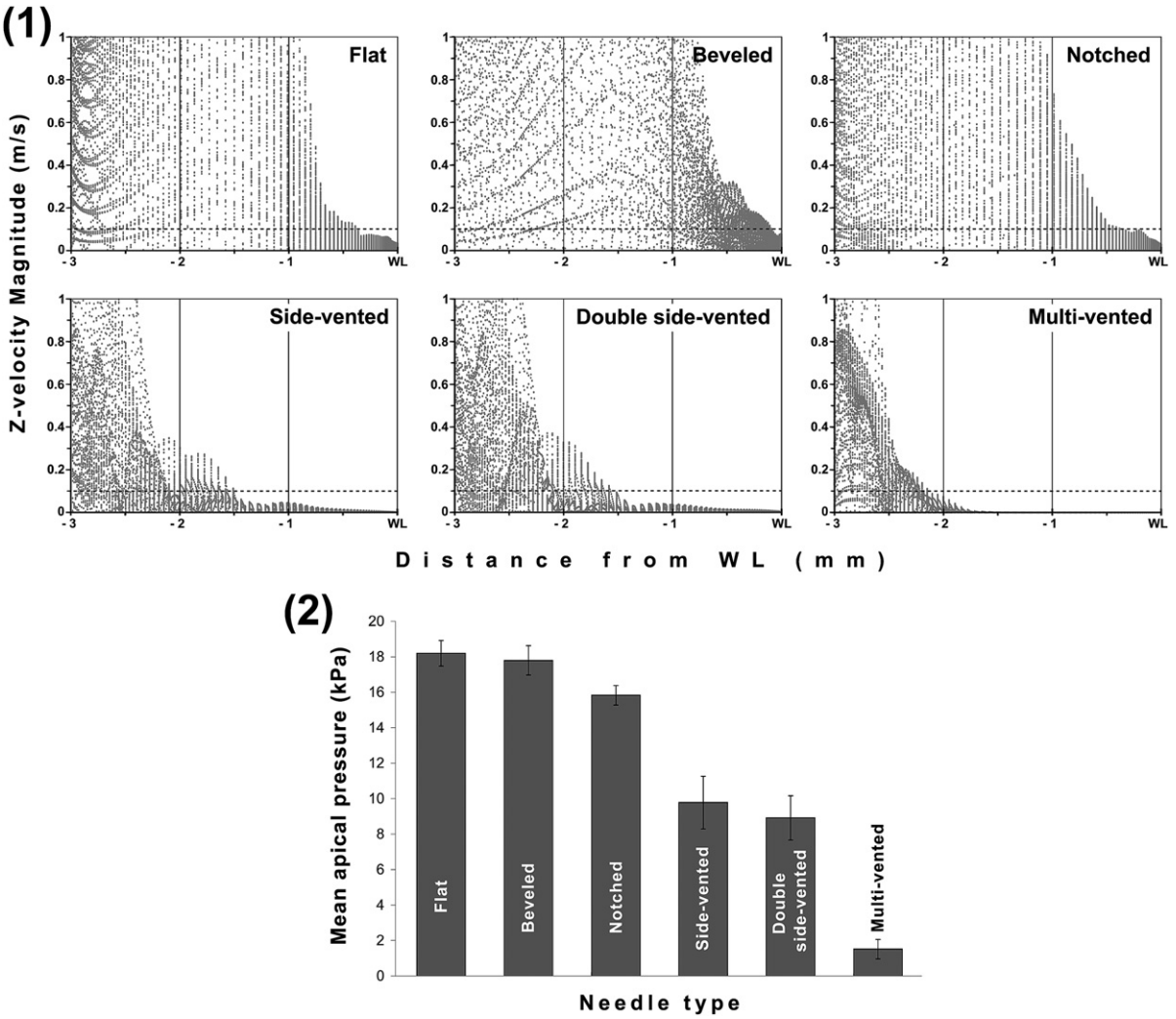

Figure 3. (1) Distribution of the axial *z* component of time-averaged irrigant velocity in the apical part of the canal as a function of distance from the WL. The scale of the vertical axis has been adjusted to 0 to 1 m/s to highlight differences in the area apically to the needle tips. Velocities higher than 0.1 m/s (horizontal stacked line) were considered clinically significant for adequate irrigant replacement. Significant replacement was evident for the flat, beveled, and notched needle more than 2.5 mm apically to the needle tip, whereas for the side-vented and double side-vented replacement was limited to within 1.5 mm. The multi-vented needle performed poorly, with irrigant replacement limited to less than 1 mm. (2) Time-averaged irrigant pressure at the apical foramen for the six needles is evaluated. Data shown as mean ± standard deviation. The flat and beveled needles led to the highest mean apical pressures. The notched needle developed a slightly lower apical pressure. The side-vented and double side-vented needles presented significantly lower apical pressure. The multi-vented needle presented the lowest apical pressure.

developed local maxima on the wall not facing the outlet (Fig. 2.3*A-C*). The side-vented and double side-vented needles led to maximum shear stress concentrated on the wall facing the outlet (the proximal outlet for the double side-vented) (Fig. 2.3*D-E*). The multi-vented needle developed the highest shear stress, but it was concentrated on a very limited area opposite to the needle outlets (Fig. 2.3*F*). Pressures developed at the apical foramen also differed among the various needle types (Fig. 3.2).

Discussion

The needles evaluated in the present study were positioned at 3 mm short of the WL. This distance was chosen based on preliminary simulations, as to create a challenging case for all needle types and allow evaluation of the flow apically to the needle tip. Therefore, it does not comprise a clinical suggestion. The effect of needle depth on the irrigant flow is going to be evaluated in a future study.

The significance of the axial *z* velocity magnitude for irrigant replacement has been discussed previously (16). Because the length of an average root canal is 20 mm and the average duration of an irrigation between successive instruments with a 30-G needle is 17.23 seconds (19), even a *z* velocity of 0.001 m/s could ideally provide some irrigant replacement. However, the streamlines are not expected to be straight from the apex to the canal orifice. Hence, such slow replacement cannot be considered adequate. Velocities in the order of 0.01 m/s could provide some effect, but velocities higher than 0.1 m/s should be considered clinically significant for adequate irrigant replacement. Nevertheless, the higher the velocity of the irrigant, the faster and more adequate the replacement is.

Shear stress on the canal wall will have an influence on the mechanical detachment of debris, tissue remnants, isolated microbes, and biofilm. Although there are no quantitative data on the minimum shear stress required, the distribution of shear stress along the canal wall provides an indication of the debridement efficacy of each needle type. It must be emphasized that the disruption or detachment of biofilm or debris cannot ensure their removal unless there is a favorable irrigant flow to carry them toward the canal orifice (reverse flow).

Even though the apical foramen was simulated as an impermeable wall, the assessment of irrigant pressure applied at this wall can give a comparative estimation of the possibility and severity of irrigant extrusion for the different needle types. We did not see any significant advantage of the notched or beveled needle over the flat needle. Furthermore, the tip of the beveled needle poses significant risks of injury for both the patient and the dentist combined with an increased possibility of wedging inside the root canal.

It has been suggested that the side-vented needle is more efficient than the beveled and notched ones in the removal of dye (10) or bioluminescent bacteria (12). These studies mainly assessed the ability of each needle to exchange the irrigant in the root canal rather than to detach debris or microbes from the wall because both the dye particles and the bioluminescent bacteria were in suspension. However, their results contradict the present finding that the irrigant exchange achieved by the side-vented needle is limited and clearly inferior to the flat, beveled, and notched needles. Limited irrigant exchange has also been reported previously for the side-vented needle (16, 20). Differences in flow rate, needle size, or depth and canal geometry could explain the different results and highlight the importance of standardizing these factors.

The reported superior performance of the side-vented needle has been attributed to turbulence (10). However, it was probably impossible to identify turbulence with the means used in that study. No turbulence was observed using a 30-G side-vented needle and a flow rate of 0.26 mL/s in both CFD and high-speed imaging studies (16, 17). The formation of vortices and unsteady flow could mistakenly have been interpreted as turbulence. In the vortex structure developed apically to the side-vented and double side-vented needle tip, the exchange of irrigant between successive vortices is expected to be limited (21). Therefore, even though the irrigant in the most apical part of the canal may be rotating inside a vortex, this does not ensure replacement.

The unidirectional performance of the side-vented and double side-vented needle has been reported previously (11, 22). In the present study, it was confirmed that the shear stress developed by these needles is significantly higher on the wall facing the outlet (the proximal one for the double side-vented needle). The second outlet of the double side-vented needle only slightly affected the overall performance and did not seem to provide any advantage, which was in agreement with a previous study (12).

Various kinds of multi-vented needles have been proposed for use during syringe irrigation (7–9). In order to recreate the needle geometry, a commercially available needle was used that is similar to multi-vented needles previously used for syringe irrigation although this needle is only recommended for use with a negative pressure system (23). The multi-vented needle appeared to be the safest type in terms of apical extrusion. On the other hand, the limited penetration and replacement of the irrigant apically necessitates placement very close to the WL, if possible less than 1 mm. An additional disadvantage was the concentration of high shear stress on a very limited area. However, these results do not reflect the efficacy of the EndoVac system because it was not designed for positive pressure irrigation.

In all cases studied, the area of high shear stress was identified in the apical part of the canal, relatively close to the tip of the needle. In this area, biofilm and debris detachment is expected to be most efficient. This finding is in agreement to a previous study that reported more efficient removal of a collagen film in the apical part of the root canal, close to the needle tip (22).

According to the results of the present study, needles that achieved improved irrigant replacement in the apical part of the root canal also led to increased mean pressure at the apical foramen, indicating an increased risk of irrigant extrusion toward the periapical tissue. From a clinical point of view, the prevention of extrusion should precede the requirement for adequate irrigant replacement and wall shear stress. Nevertheless, the effect of additional factors such as needle depth, root canal size, and taper should be evaluated before any clinical suggestion on the supremacy of a particular needle type. In conclusion, the flow pattern of the open-ended needles was different from the close-ended needles resulting in more irrigant replacement in front of the open-ended needles but also higher apical pressure.

Acknowledgments

We thank B. Benschop for technical assistance. Needles were kindly provided by KerrHawe SA, Transcodent GmbH & Co, KG, and Vista Dental.

Supplementary data

Videos accompany the on-line version of this article (available at http://www.aae.org).

References

1. Haapasalo M, Endal U, Zandi H, et al. Eradication of endodontic infection by instrumentation and irrigation solutions. Endod Top 2005;10:77–102.
2. Ingle JI, Himel VT, Hawrish CE, et al. Endodontic cavity preparation. In: Ingle JI, Bakland LK, eds. Endodontics. 5th ed. Ontario, Canada: BC Decker; 2002:502.
3. Peters OA. Current challenges and concepts in the preparation of root canal systems: a review. J Endod 2004;30:559–67.
4. Senia ES, Marshall JF, Rosen S. The solvent action of sodium hypochlorite on pulp tissue of extracted teeth. Oral Surg Oral Med Oral Pathol 1971;31:96–103.
5. Vande Visse JE, Brilliant JD. Effect of irrigation on the production of extruded material at the root apex during instrumentation. J Endod 1975;1:243–6.
6. Ram Z. Effectiveness of root canal irrigation. Oral Surg Oral Med Oral Pathol 1977; 44:306–12.
7. Goldman M, Kronman JH, Goldman LB, et al. New method of irrigation during endodontic treatment. J Endod 1976;2:257–60.
8. Goldman LB, Goldman M, Kronman JH, et al. Scanning electron microscope study of a new irrigation method in endodontic treatment. Oral Surg Oral Med Oral Pathol 1979;48:79–83.
9. Moser JB, Heuer MA. Forces and efficacy in endodontic irrigation systems. Oral Surg Oral Med Oral Pathol 1982;53:425–8.
10. Kahn FH, Rosenberg PA, Gliksberg J. An in vitro evaluation of the irrigating characteristics of ultrasonic and subsonic handpieces and irrigating needles and probes. J Endod 1995;21:277–80.
11. Yamamoto A, Otogoto J, Kuroiwa A, et al. The effect of irrigation using trial-manufactured washing needle. Jap J Cons Dent 2006;49:64–70.
12. Vinothkumar TS, Kavitha S, Lakshminarayanan L, et al. Influence of irrigating needle-tip designs in removing bacteria inoculated into instrumented root canals measured using single-tube luminometer. J Endod 2007;33:746–8.
13. Hülsmann M, Rödig T, Nordmyer S. Complications during root canal irrigation. Endod Top 2009;16:27–63.
14. Tilton JN. Fluid and particle dynamics. In: Perry RH, Green DW, Maloney JO, eds. Perry's Chemical Engineer's Handbook. 7th ed. New York, NY: McGraw-Hill; 1999:1–50.
15. Arvand A, Hormes M, Reul H. A validated computational fluid dynamics model to estimate hemolysis in a rotary blood pump. Artif Org 2005;29:531–40.
16. Boutsioukis C, Lambrianidis T, Kastrinakis E. Irrigant flow within a prepared root canal using different flow rates: a computational fluid dynamics study. Int Endod J 2009;42:144–55.
17. Boutsioukis C, Verhaagen B, Versluis M, et al. Irrigant flow in the root canal: experimental validation of an unsteady computational fluid dynamics model using high-speed imaging. Int Endod J (in press).
18. Boutsioukis C, Lambrianidis T, Vasiliadis L. Clinical relevance of standardization of endodontic irrigation needle dimensions according to the ISO 9626:1991 & 9626:1991/Amd 1:2001 specification. Int Endod J 2007;40:700–6.
19. Boutsioukis C, Lambrianidis T, Kastrinakis E, et al. Measurement of pressure and flow rates during irrigation of a root canal ex vivo with three endodontic needles. Int Endod J 2007;40:504–13.
20. Zehnder M. Root canal irrigants. J Endod 2006;32:389–98.
21. Shankar PN, Deshpande MD. Fluid mechanics in the driven cavity. Annu Rev Fluid Mech 2000;32:93–136.
22. Huang TY, Gulabivala K, Ng YL. A bio-molecular film ex-vivo model to evaluate the influence of canal dimensions and irrigation variables on the efficacy of irrigation. Int Endod J 2008;41:60–71.
23. Discus Dental: EndoVac® Apical Negative Pressure Irrigation System: Directions for use. Culver City, CA: Discus Dental; 2009:1–2.